Comparison Study on Pyrolysis Characteristics and Kinetics of Corn Stover and Its Digestate by TG-FTIR

Deli Zhang,[a,b] Fang Wang,[a,b] Weiming Yi,[a,b,*] Zhihe Li,[a,b] Xiuli Shen,[a,b] and Weisheng Niu [c]

The pyrolysis potential of corn stover digestate (CSD) was compared with corn stover (CS). The effects of anaerobic digestion (AD) on pyrolysis were investigated at different rates by a thermogravimetric analyzer coupled with Fourier transform infrared spectrometry (TG-FTIR). The distributed activation energy model (DAEM) was used to show the differences in the kinetics. The results indicated that the AD process improved the thermal stability with lower mean reactivity (R_M), higher solid residue (S_{850}), and decreased release of observed gaseous productions, except for CH_4. The release of CH_4 from CSD was higher than that of CS, especially in the temperature range of 430 °C to 520 °C. The activation energies (E) of CS and CSD were 184 kJ/mol to 293 kJ/mol (conversions were 0.1 to 0.8) and 99 kJ/mol to 331 kJ/mol (conversions were 0.1 to 0.9), respectively. The activation energies decreased after AD at the same conversion level. The calculated TG data of CS and CSD from the kinetic parameters were in good agreement with the experimental curves.

Contact information: a: School of Agricultural Engineering and Food Science, Shandong University of Technology, Zibo, Box 255049, China; b: Shandong Research Center of Engineering and Technology for Clean Energy, Zibo, Box 255049, China; c: College of Engineering, Shenyang Agricultural University, Shenyang, Box 110866, China; *Corresponding author: yiweiming@sdut.edu.cn

INTRODUCTION

Anaerobic digestion (AD) of biomass is a promising technology for energy utilization and environmental protection. AD plants are typically used to produce heat and electricity through the combined heat power (CHP) system or as a natural gas source. Due to the rich contents of nutrients and fibrillar components, the digestate of AD plants is mainly applied for fertilizer. The supplies of the digestate are sustained, but the demands of the soil and vegetation are seasonal. With the excessive accumulation of the residues, the contradiction between supply and demand has become more serious. Moreover, due to the remaining heavy metal, pathogenic bacteria, and antibiotics in the residues, there is potential environmental pollution and harm to the human body caused by digestate. Therefore, more ways to utilize the digestate are needed (Monlau *et al.* 2015a; Fabbri and Torri 2016).

Pyrolysis technology could convert biomass to biofuels or biomaterials in high temperature without oxygen. Previous studies have indicated the potential advantages of using pyrolysis with the digestate as a feedstock. Liang *et al.* (2015) showed that the selectivity of pyrolytic products with phenols could be improved by AD, especially for the yield of 4-vinylphenol. Similar conclusions were reported by Wang *et al.* (2016) in the bio-pretreatment of methanogen. Neumann *et al.* (2016) discussed a novel

combination that had a digestate and thermo-catalytic reforming process that was used to improve the quality of the bio-oil with low viscosity and acid number; its calorific value was 35.2 mJ/kg. Inyang *et al.* (2010) considered the influence of AD on biochar property, showing that the bio-char derived from digestate was superior for soil amelioration, contaminant remediation, or wastewater treatment compared with raw materials. The phosphate and heavy metal removal potential of digestate derived bio-char is comparable to commercial activated carbons (Yao *et al.* 2011; Inyang *et al.* 2012). The energy recovery with pyrolysis of digestate is enhanced compared with AD alone. Additionally, a 6.1 MJ/kg VS energy yield was achieved from the pyrolysis of digestate from chicken manure and corn stover (Li *et al.* 2014). Monlau *et al.* (2015b) estimated that the digestate pyrolysis increased the production of electricity by 42% compared with the AD stand-alone plant based on a full scale AD plant. However, most studies on biogas residue pyrolysis have focused on the features and applications of productions and energy efficiency analysis. Few detailed studies have investigated the behaviors of evolved gases in real time during pyrolysis. Li *et al.* (2017) showed that AD had discriminative effects on pyrolysis kinetics for sludge, food waste, vinasse, and cow manure. Hence, it is indispensable to consider the thermal degradation and kinetics compared with corn stover (CS) and its digestate (CSD), which are some of the main resources for AD plants. These gas release characteristics and kinetics are helpful to approach the pyrolysis mechanism of biogas digestate.

Thermogravimetric analysis coupled with Fourier transform infrared spectrometry (TG-FTIR) has been widely used to examine the pyrolysis of biomass such as lignocellulose, marine algae, and their derived components (Wang *et al.* 2014; Ceylan and Goldfarb 2015; Tian *et al.* 2016). This combined method monitors the mass loss of materials with a constant heating rate and distinguishes the functional groups of volatiles during pyrolysis in real time. In addition, the study of kinetics is an important part of biomass pyrolysis. Numerous kinetic analysis models have been reported in the thermal analysis. The distributed activation energy model (DAEM) computing method was improved by Miura (1995) and is widely applied for biomass to show the relationships between activation energy and conversions (Cai *et al.* 2013; Cao *et al.* 2014; Soria-Verdugo *et al.* 2014).

The objective of this paper was to support the application of CSD on pyrolysis. The weight loss characteristics and gas evolution rules for CS and CSD were investigated to explore the effects of AD on the pyrolysis by TG-FTIR. The DAEM method was used to analyze the pyrolysis kinetics of CSD compared with CS. Additionally, the changes in the physicochemical properties between CS and CSD were considered. The research is advantageous in the further applications of pyrolysis or in other thermal conversion technology linked with the AD process.

EXPERIMENTAL

Materials

CSD was prepared from a batch of AD at 35 °C for 35 d. The mass ratio of substrates and the inoculum was a 7:3 based on the total solid (TS) content at 10%. The CS was collected from Zibo in the district of Shandong Province. Before the analysis, the CS and CSD were pulverized to particle sizes below 1 mm and dried at 80 °C for 24 h.

Elemental and Lignocellulosic Analysis

The elemental composition of CHNS was conducted on an elemental analyzer (Vario EL cube, Langenselbold, Germany), and the oxygen content was accounted by difference. The cellulose, hemicellulose, and lignin contents were determined by an extraction unit (FIWE6, VELP Co., Usmate, Italy), following the procedure developed by Van Soest *et al.* (1991).

TG-FTIR Analysis

A thermogravimetric analyzer (TA Instruments, New Castle, USA) coupled with Fourier transform infrared spectrometry (Thermo Scientific Nicolet iS 50, Waltham, Ma, USA) was used to study the pyrolysis behaviors and kinetics parameters of CS and CSD. The experiments operated from 30 °C to 850 °C under heating rates of 10, 20, and 30 °C/min. The carrier gas was high-purity nitrogen flowing at 60 mL/min to ensure the inert gas atmosphere. The temperature was maintained at 210 °C in the transfer line between the two instruments. The spectrum range of the FTIR was 4000 cm^{-1} to 400 cm^{-1}, and the resolution was 2 cm^{-1}. A total of 8 ± 0.05 mg of sample was used with each experiment to reduce the variation caused by sample amount.

Analysis of Kinetic Parameters

In the model of DAEM, the reaction consisted of a series of irreversible and independent first-order parallel reactions following the continuous function distribution. The change in total volatiles at different temperature was represented as follows (Miura 1995),

$$1 - V / V^* = \int_0^\infty \Phi(E, T) f(E) dE \tag{1}$$

$$\Phi(E, T) = \exp(-\frac{k_0}{\alpha} \int_0^T e^{-E/RT} dT) \tag{2}$$

where V is the volatile content at temperature T, V^* is the effective volatile content, k_0 is the frequency factor corresponding to the E value, α is the heating rate, and $f(E)$ is the distribution curve of the activation energy. The distribution curve $f(E)$ is normalized to satisfy Eq. 3.

$$\int_0^\infty f(E) dE = 1 \tag{3}$$

In this study, the kinetic parameters were estimated by the integral method proposed by Miura and Maki (1998). Equation 1 was simplified to Eq. 4,

$$V / V^* \cong 1 - \int_{E_s}^\infty f(E) dE = \int_0^{E_s} f(E) dE \tag{4}$$

where E_s is chosen to satisfy $\Phi(E_s, T) = 0.58$ at a given temperature. Both activation energy (E) and pre-exponential (k_0) factor can be estimated by the Arrhenius equation (Eq. 5); the slope and intercept of the Arrhenius plot are used to calculate the E and k_0, respectively.

$$\ln(\frac{\alpha}{T^2}) = \ln(\frac{k_0 R}{E}) + 0.6075 - \frac{E}{R}\frac{1}{T} \tag{5}$$

To predict TG curves with the kinetic parameters calculated from the DAEM, the method used by Ceylan and Kazan (2015) and Li *et al.* (2017) was adopted. A linear equation is expressed as follows,

$$\ln(1 / T^2) = m / T + n \tag{6}$$

where m and n are the slope and the intercept of the plots of $\ln(1/T^2)$ versus $1/T$ at a given heating rate.

An expression to calculate temperature with different conversion rates can be determined by Eq. 5 and Eq. 6 simultaneously as Eq. 7.

$$T = \frac{m + \dfrac{E}{R}}{\ln(k_0 R / E) + 0.6075 - (\ln \alpha + n)} \tag{7}$$

Plots of V/V^* versus T from DAEM data were compared with experimental data.

RESULTS AND DISCUSSION

Properties of CS and CSD

The AD process changed the elemental contents and components of CS. As shown in Table 1, the carbon content was increased slightly. The oxygen was decreased noticeably, which is favorable for feedstock that is transformed into high-quality bio-oil with pyrolysis (Cen *et al.* 2016). The crystalline regions of cellulose and the presence of lignin were the main obstacles for the biodegradation of lignocellulose. Since hemicellulose contains more branch chains and amorphous region, it biodegraded more easily than cellulose. And the lignin was almost undegraded in anaerobic conditions. Therefore, the content of hemicellulose and cellulose decreased by 36.2% and 25.2%, respectively. The lignin content increased from 7.04% to 16.86%. The biodegradation of CS led to the variation of the element. In addition, the content of ash increased from 3.92% to 11.59%, which was caused by the addition of salt additives and the concentration effect in biogas residue with AD.

**Table 1.** Ultimate and Lignocellulosic Analysis of CS and CSD

Sample	Ultimate Composition (db, wt.%)					Lignocellulosic Composition (db, wt.%)			
	C	H	O	N	S	Ash	Cellulose	Lignin	Hemicellulose
CS	39.95	4.23	50.16	1.34	0.40	3.92	42.85	7.04	29.39
CSD	41.55	4.99	39.25	2.09	0.53	11.59	32.04	16.86	18.75

Thermogravimetric Analysis of CS and CSD

Figure 1 shows the thermogravimetric (TG) and derivative thermogravimetric (DTG) curves of CS and CSD under 30 °C/min. The thermal weight loss was divided into three stages within the temperature range of 30 °C to 850 °C according to the peak of the DTG curves; the stages were moisture evaporation and slight degradation, main pyrolysis, and carbonization.

The weight losses of two samples in the first stage were 6.6 and 7.8%, corresponding to the moisture content of the samples. There were noticeable differences in the second stage during the temperature range of 230 °C to 550 °C between CS and CSD, with a weight loss of 64.5% and 50.6%, respectively. The maximum weight loss rate (D_{max}) of CS was much higher than CSD, which was attributed to the changes of compositions in AD process. The pyrolysis characteristics of the three main components

were different, the degradation of cellulose and hemicellulose occurred more quickly, and the lignin had a wider pyrolysis temperature range (Quan *et al.* 2016). Moreover, there was a stronger shoulder peak in the DTG curve of CS than that of CSD, which could be explained by the degradation of hemicellulose in the AD process (Skodras *et al.* 2006).
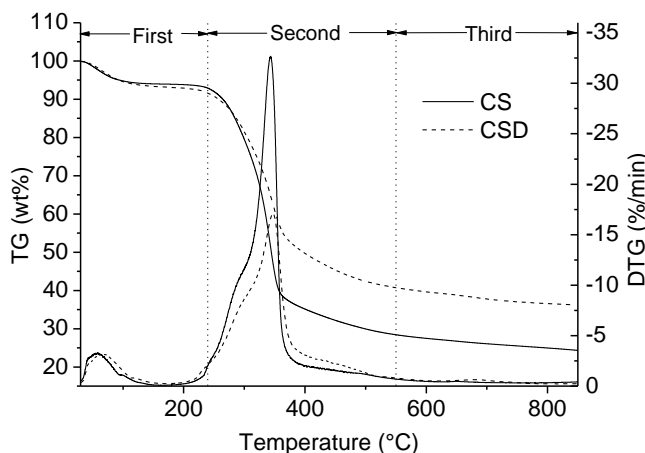
Fig. 1. Weight loss and derivative weight loss curves for CS and CSD

In the carbonization stage, there was a slight weight loss in CS and CSD of 5.6% and 6.1%, respectively. The solid residue that was at 850 °C temperature (S_{850}) of CSD was higher than CS. This result agreed with the changes of components in the course of AD process. The pyrolytic parameters of CS and CSD are shown in Table 2. Mean reactivity (R_M) was used to describe the pyrolysis reactivity based on the method in Ghetti *et al.* (1996), which was defined as the ratio of D_{max} and T_{max} for the pyrolysis peak of the second stage. The lower value of R_M and higher value of S_{850} in CSD implied that the AD process inhibited the thermal volatile release of CS.

**Table 2.** Pyrolytic Parameters of CS and CSD

Samples	D_{max} (% min⁻¹)	T_{max} (°C)	S_{850} (%)	R_M (% min⁻¹ °C⁻¹)
CS	32.67	343	24.3	0.095
CSD	17.10	347	36.2	0.049

Compared with CS, a visible change was observed in the TG-DTG curves of CSD. The AD improved the thermal stability of CS. This result was attributed to the decrease in cellulose and hemicellulose contents and the increase of the relative content of lignin. The increase in ash content was also a potential factor. Alkaline and alkaline earth metals promote the formation of char during biomass pyrolysis (Fahmi *et al.* 2007).

FTIR Analysis of Pyrolysis

The emission of gases during the pyrolysis of CS and CSD under 30 °C min⁻¹ is shown in Fig. 2, where the distribution of absorbance at different temperatures was in agreement with the DTG curves. The tendency of both samples was similar, but the absorption intensity of CSD was weakened. The characteristic absorptions of the volatiles are listed in Table 3 and Fig. 3 (Tihay and Gillard 2010; Chen *et al.* 2015; Lazdovica *et al.* 2017). Only a small portion of low molecules and organic volatiles were released at 240 °C at the initiation of main pyrolysis stage. As the temperature increased, the gas production increased with an intensification of pyrolytic degradation, as shown in Fig.

***bioresources*.com**

3(b). At 345 °C, which was approximately the maximum weight loss temperature, abundant and complex organic volatiles were released, including carbonyl groups and oxhydryl groups, which represent the carboxylic, ketone, aldehyde, alcohols, and levoglucosan (LG). CO_2 is the primary component of incondensable gases. However, with the temperature further increasing, the organic volatiles almost disappeared as shown in Fig. 3(d). And, slight CO_2 and CH_4 were observed, caused by cracking of C-H and C-O bonds and aromatization reactions.
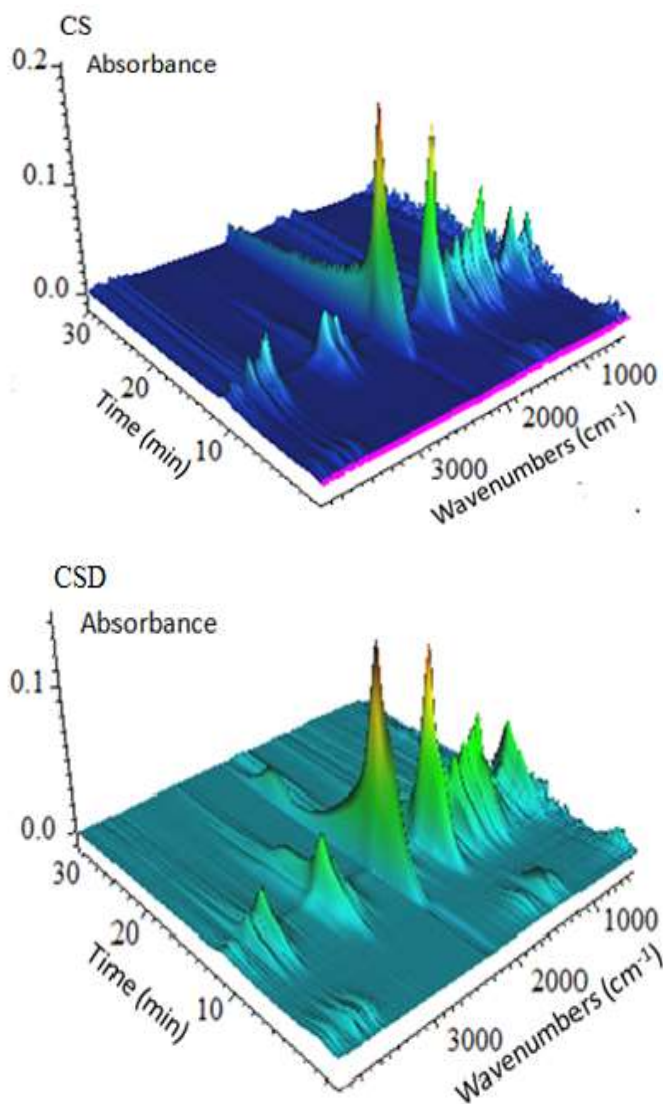
Fig. 2. 3-D TG-FTIR diagram of CS and CSD pyrolysis at 30 °C/min
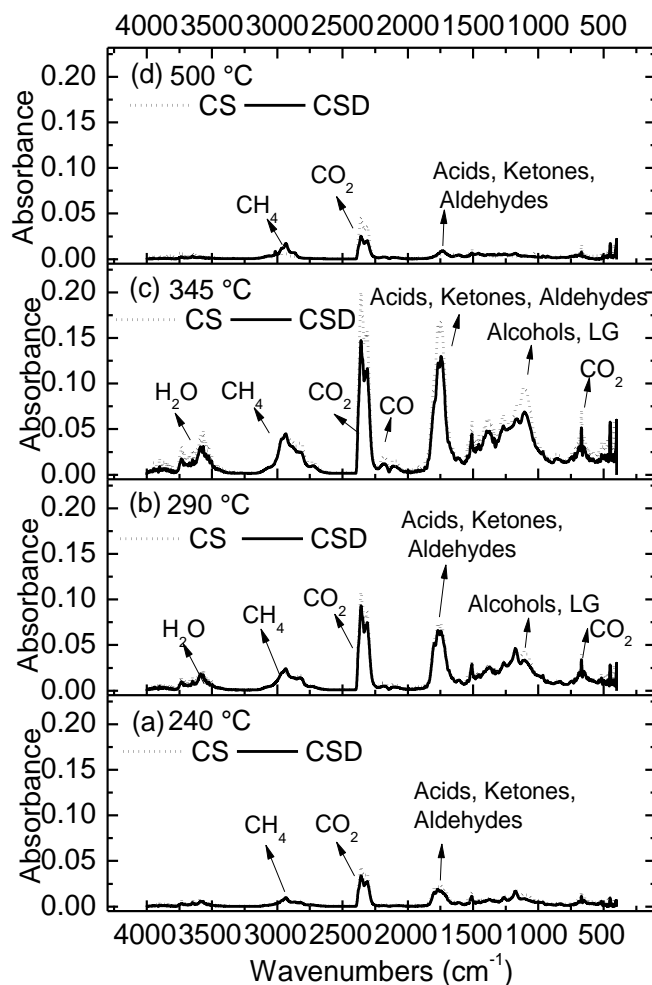
Fig. 3. FTIR spectrum of evolved gases during pyrolysis for CS and CSD at 30 °C/min

The TG-FTIR test conditions of CS and CSD were identical, so the change in absorbance for a given wavenumber was linear with the corresponding gas yield according to Beer-Lambert law (Gao *et al.* 2013). The evolution of absorbance intensity of gaseous components is shown in Fig. 4; the components were identified by their characteristic bands listed in Table 3.

Table 3. Characteristic IR Spectra Absorptions of the Volatiles

| Wave Numbers (cm^{-1})	Functional Groups (Vibrations)	Components	Peak (cm^{-1})	
			CS	CSD
4000 to 3400	O-H (Stretching)	H_2O	3566	3566
3000 to 2842	C-H (Stretching)	CH_4	2943	2934
2400 to 2250	C=O (Stretching)	CO_2	2358	2358
2250 to 2000	C-O (Stretching)	CO	2184	2184
1800 to 1684	C=O (Stretching)	Acids, Ketones, Aldehydes	1745	1745
1131 to 1058	C-O-H (Stretching)	Alcohols, Levoglucosan	1107	1105

The evolution profile of the CO_2 from CSD appeared in two peaks, where the higher peak occurred at 347 °C and the lower peak at 682 °C. The evolution profile was different in CS where there was only one peak. At a low temperature, CO_2 mainly

originated from the primary decomposition of hemicellulose through decarboxylation and decarbonylation. The further fracture of the C-O and carboxyl groups of lignin were the main sources of CO_2 production at high temperature (Yuan *et al.* 2015). The second peak of CSD was possibly caused by the degradation of lignin. The evolution curves of CO for both CS and CSD had a sharp peak and reached a maximum at approximately 350 °C. After approximately 600 °C, the release of CO increased relatively slowly. According to Fu *et al*. (2012), the CO released below 450 °C was formed by the cracking of ether and carbonyl groups. At high temperatures (> 600 °C), CO was mainly produced from the secondary pyrolysis of char decomposition (Yang *et al.* 2007), which caused the CS to have a higher curve. The H_2O evolution of both CS and CSD exhibited two peaks. The two peaks were mainly caused by the evaporation of free water and the dehydroxylation of carbohydrates, respectively.

Compared with CS, the release of CO_2, CO, and H_2O from CSD was much weaker. Below 400 °C, the phenomenon was attributed to the lower contents of cellulose and hemicellulose of CSD caused by AD. When the temperature was higher than 400 °C, the weaker intensity of the secondary pyrolysis of organic volatiles may be the reason for the appearances.

The FTIR profiles of CH_4 from both CS and CSD showed a complete peak and a shoulder peak at approximately 400 °C and 500 °C, respectively. This pattern was different from other gaseous components where the first peak of CSD was slightly higher than that of CS. The second peak of CSD was approximately 2.5 times higher from 430 °C to 520 °C, which stayed consistent with the ratio of lignin content in Table 1. Lignin is the primary source for CH_4. The first peak was mainly generated from the cleavage in lignin side chains, while the second peak was attributed to the profound rupture of aromatic rings and/or secondary pyrolysis (Wang *et al.* 2009). Based on the research of De La Cruz F. *et al.* (2014), methoxy groups in phenol moieties are degraded under AD, which could explain the slight difference in the low temperature peak in CH_4 at low temperatures.

The characteristic absorbances in the C=O stretching vibration related to acids, ketones, and aldehydes were found at 1800 cm^{-1} to 1684 cm^{-1}. The C-O-H stretching vibration related to alcohols and LG were found at 1131 cm^{-1} to 1058 cm^{-1}. According to Gao *et al.* (2010), acids, ketones, and aldehydes were mainly produced by hemicellulose and cellulose pyrolysis, especially in the hemicelluloses. After the AD process, cellulose and hemicellulose degradation decreased the carbonyl organic compounds. The same reason could be used to explain the reduction in alcohols and LG that were mainly from cellulose pyrolysis. In addition, the lower organic release was one reason for the lower secondary pyrolysis of CSD.
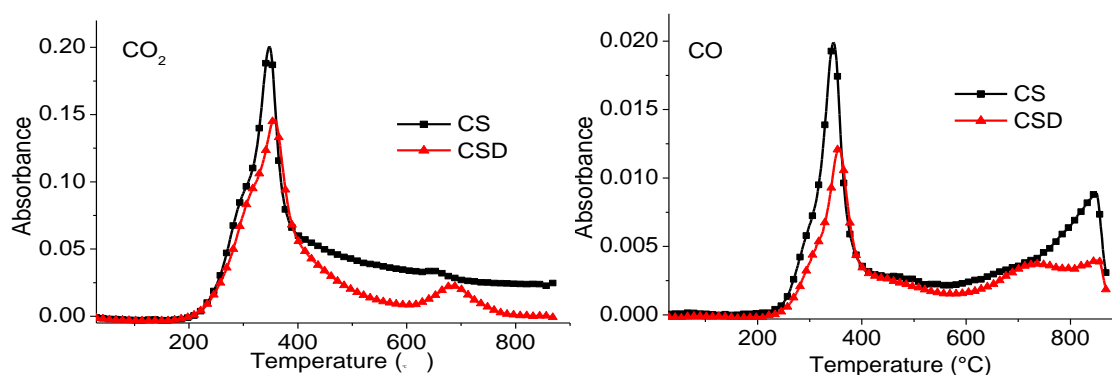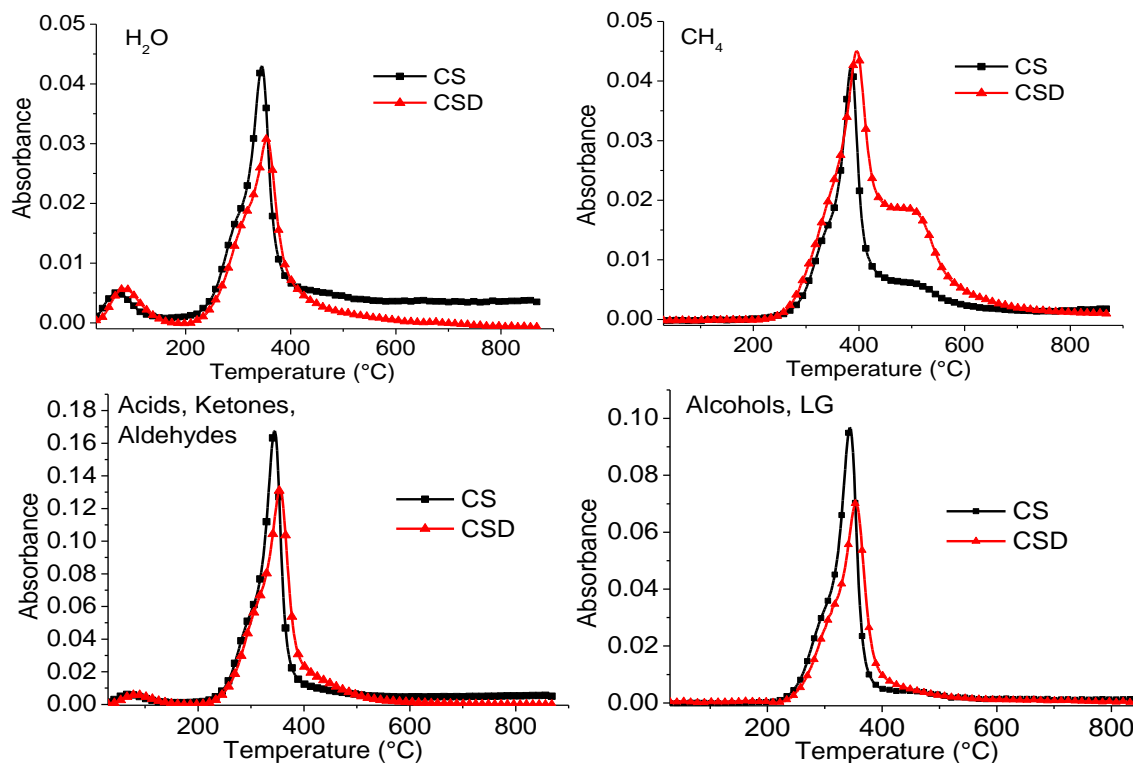
**Fig. 4.** Comparison of pyrolysis product evolution curves for CS and CSD

Kinetic Analysis

Three different heating rates ranging from 10 °C/min to 30 °C/min were used to deduce the dependence of activation energy (E) with the conversions during pyrolysis. Because the coefficient of determination (R^2) of the CS fitting curve at the conversion of 0.9 was rather low, the corresponding activation energy was ignored. Meanwhile, the other R^2 of the lines drawn at various conversions were greater than 0.95, indicating it was well fitted by the method. Hence, CS conversions varying from 0.1 to 0.8 and 0.1 to 0.9 of CSD were considered in this study. The regression lines for Arrhenius plots of $\ln(\alpha/T^2)$ and $1/T$ are shown in Fig. 5. According to Eq. 5, the E and k_0 at different levels of conversions V/V^* were estimated from the slope and intercept of all lines.
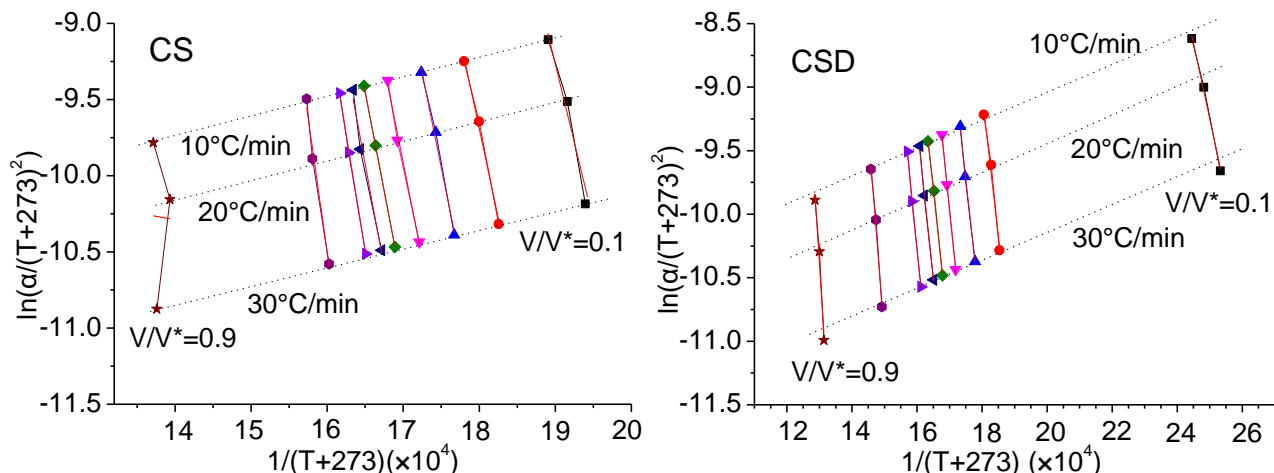
Fig. 5. Arrhenius plot of ln (α/T^2) vs. $1/T$ at selected V/V^* values for CS and CSD

The activation energy variation ranged from 184 kJ/mol to 293 kJ/mol for CS and 99 kJ/mol to 331 kJ/mol for CSD, as shown in Fig. 6. These values were inconsistent with those of corn stover, groundnut shell, and cotton husk (Ma *et al.* 2013; Bhavanam and Sastry 2015). The pre-exponential factors for the corresponding activation energies were calculated to be in the order of 10^{16} to 10^{24} in CS and 10^{12} to 10^{22} in CSD.
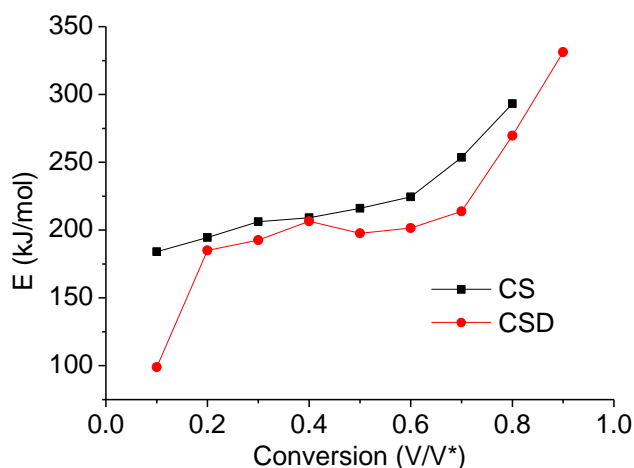
Fig. 6. *E vs. V/V** estimated from the Arrhenius plot for CS and CSD

With the increase in conversion, the activation energy curves of both samples increased; in particular, a sharp raise appeared when the conversion values were higher than 0.7. The *E* of CSD at 0.1 conversion was remarkably lower than CS, which is attributed to the low corresponding temperature of approximately 130 °C. The *E* values of CSD pyrolysis were lower than that of CS at the same conversion level, indicating that the AD process reduced the activation energy of CS.

A reaction with lower apparent activation energy requires less energy to break down the chemical bonds between atoms (Ceylan and Kazan 2015). So the lower *E* of CSD was favorable for pyrolysis. Similar trends were reported by Li *et al.* (2017) using the AD substrates of lignocellulose biomass, vinasse, and cow manure. The phenomenon is possible caused by the increase in the proportion of lignin and ash. The activation

energy of lignin is lower than that of cellulose and hemicellulose (Manya *et al.* 2003; Barneto *et al.* 2010); alkaline salts in biomass, whether added or innate, reduce the activation energy (Nassar 1999).

To predict TG curves, the values of *m* and *n* were obtained with Eq. 6, as shown in Fig. 7. All of the R^2 were higher than 0.98. Using Eq. 7, the experimental curves and the calculated plots of the conversion *V/V* vs. T* of CS and CSD at 30 °C/min were compared in Fig. 8. The DAEM plots were in well agreement with the experimental data implying a favorable validity of kinetic analysis.
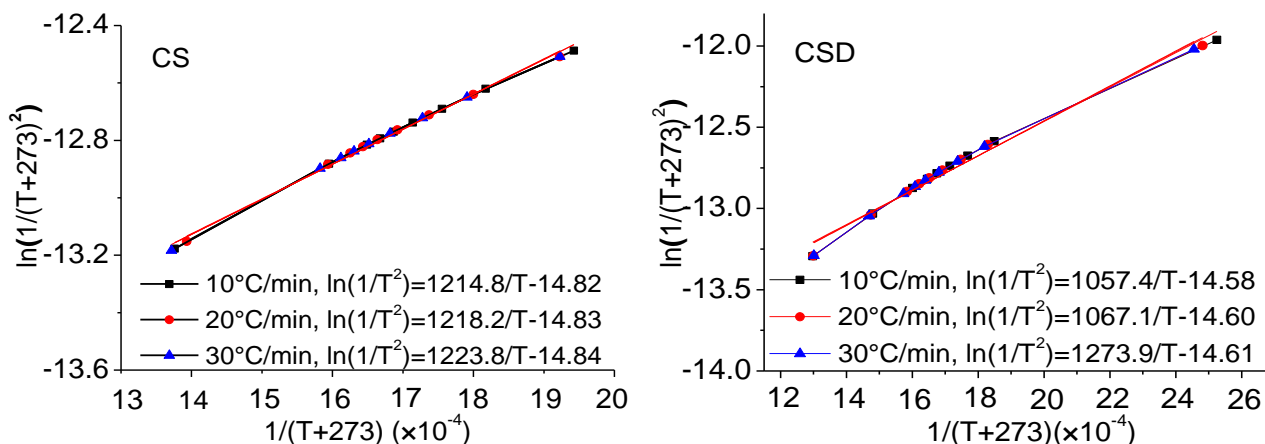

Fig. 7. Linearization of $\ln(1/T^2)$ *vs.* $1/T$ curves for different heating rates of CS and CSD (10, 20, and 30 °C/min)
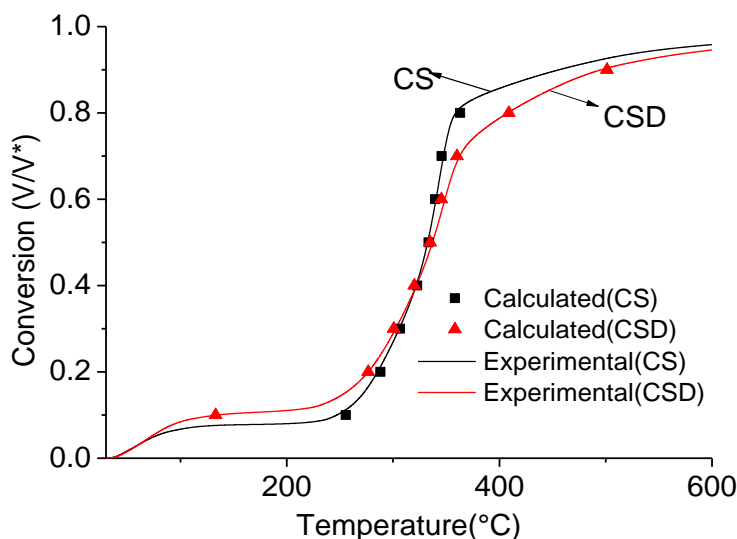

Fig. 8. Comparison of experimental curves and calculated plots for CS and CSD

CONCLUSIONS

1. The anaerobic digestion (AD) process changed the components of corn stover (CS) and led to a visible change in the TG-DTG curves. The mean reactivity (R_M) decreased from 0.095 to 0.049% min^{-1} °C^{-1}, and the solid residue (S_{850}) increased

bioresources.com

from 24.3% to 36.2%. Thus, the AD improved the thermal stability of CS.

2. Compared with CS, the release of gaseous products from corn stover digestate (CSD) were reduced, including CO_2, CO, H_2O, and various organic volatiles. However, the release of CH_4 was increased, especially within the temperature range from 430 °C to 520 °C, where the product was improved by approximately 2.5 times. A possible explanation is the modifications in the lignin from the AD.

3. The activation energies (E) of CS and CSD were 184 kJ/mol to 293 kJ/mol and 99 kJ/mol to 331 kJ/mol at the conversions from 0.1 to 0.8 and 0.1 to 0.9, respectively. They had a similar E distribution where they rose as the temperature increased. However, the E distribution of the CSD was lower than the CS at the same conversion level. The kinetic parameters calculated by the distributed activation energy model (DAEM) were properly fitted with the experimental devolatilization curves.

4. The lower E distribution and better thermal stability compared to CS indicated that the CSD was favorable for pyrolysis with the target product of char.

ACKNOWLEDGMENTS

REFERENCES CITED

Barneto, A. G., Carmona, J. A., Alfonso, J. E., and Serrano, R. S. (2010). "Simulation of the thermogravimetry analysis of three non-wood pulps," *Bioresource Technology* 101(9), 3220-3229. DOI: 10.1016/j.biortech.2009.12.034

Bhavanam, A., and Sastry, R. C. (2015). "Kinetic study of solid waste pyrolysis using distributed activation energy model," *Bioresource Technology* 178, 126-131. DOI: 10.1016/j.biortech.2014.10.028

Cai, J., Wu, W., Liu, R., and Huber, G. W. (2013). "A distributed activation energy model for the pyrolysis of lignocellulosic biomass," *Green Chemistry* 15, 1331-1340. DOI: 10.1039/C3GC36958G

Cao, H., Xin, Y., Wang, D., and Yuan, Q. (2014). "Pyrolysis characteristics of cattle manures using a discrete distributed activation energy model," *Bioresource Technology* 172, 219-225. DOI: 10.1016/j.biortech.2014.09.049

Cen, K., Chen, D., Wang, J., Cai, Y., and Wang, L. (2016). "Effects of water washing and torrefaction pre-treatments on corn stalk pyrolysis: Combined study using TG-FTIR and a fixed bed reactor," *Energy & Fuels* 30(12), 10627-10634. DOI: 10.1021/acs.energyfuels.6b02813

Ceylan, S., and Goldfarb, J. L. (2015). "Green tide to green fuels: TG–FTIR analysis and kinetic study of *Ulva prolifera* pyrolysis," *Energy Conversion and Management* 101, 263-270. DOI: 10.1016/j.enconman.2015.05.029

Ceylan, S., and Kazan, D. (2015). "Pyrolysis kinetics and thermal characteristics of

bioresources.com

microalgae *Nannochloropsis oculata* and *Tetraselmis sp.*," *Bioresource Technology* 187, 1-5. DOI: 10.1016/j.biortech.2015.03.081

Chen, L., Wang, X. H., Yang, H. P., Lu, Q., Li, D., Yang, Q., and Chen, H. P. (2015). "Study on pyrolysis behaviors of non-woody lignins with TG-FTIR and Py-GC/MS," *Journal of Analytical and Applied Pyrolysis* 113, 499-507. DOI: 10.1016/j.jaap.2015.03.018

De La Cruz, F. F. B., Yelle, D. J., Gracz, H. S., and Barlaz, M. A. (2014). "Chemical changes during anaerobic decomposition of hardwood, softwood, and old newsprint under mesophilic and thermophilic conditions," *Journal of Agricultural and Food Chemistry* 62(27), 6362-6374. DOI: 10.1021/jf501653Hc

Fabbri, D., and Torri, C. (2016). "Linking pyrolysis and anaerobic digestion (Py-AD) for the conversion of lignocellulosic biomass," *Current Opinion in Biotechnology* 38, 167-173. DOI: 10.1016/j.copbio.2016.02.004c

Fahmi, R., Bridgwater, A. V., Darvell, L. I., Jones, J. M., Yates, N., Thain, S., and Donnison, I. S. (2007). "The effect of alkali metals on combustion and pyrolysis of Lolium and Festuca grasses, switchgrass and willow," *Fuel* 86, 1560-1569. DOI: 10.1016/j.fuel.2006.11.030

Fu, P., Hu, S., Xiang, J., Sun, L. S., Su, S., and An, S. (2012). "Study on the gas evolution and char structural change during pyrolysis of cotton stalk," *Journal of Analytical and Applied Pyrolysis* 97, 130-136. DOI: 10.1016/j.jaap.2012.05.012

Gao, N. B., Li, A. M., Quan, C., and Duan, Y. (2013). "TG–FTIR and Py–GC/MS analysis on pyrolysis and combustion of pine sawdust," *Journal of Analytical and Applied Pyrolysis* 100, 26-32. DOI: 10.1016/j.jaap.2012.11.009

Gao, L., Wu, S., and Lou, R. (2010). "Characteristics of corn stalk hemicellulose pyrolysis in a tubular reactor," *BioResources* 5(4), 051-2062. DOI: 10.15376/biores.5.4.2051-2063

Ghetti, P., Ricca, L., and Angelini, L. (1996). "Thermal analysis of biomass and corresponding pyrolysis products," *Fuel* 75(5), 565-573. DOI: 10.1016/0016-2361(95)00296-0

Inyang, M., Gao, B., Yao, Y., Xue, Y. W., Zimmerman, A. R., Pullammanappallil, P., and Cao, X. D. (2012). "Removal of heavy metals from aqueous solution by biochars derived from anaerobically digested biomass," *Bioresource Technology* 110, 50-56. DOI: 10.1016/j.biortech.2012.01.072C

Inyang, M., Gao, B., Pullammanappallil, P., Ding, W., and Zimmerman, A. R. (2010). "Biochar from anaerobically digested sugarcane bagasse," *Bioresource Technology* 101(22), 8868-8872. DOI: 10.1016/j.biortech.2010.06.088

Miura, K. (1995). "A new and simple method to estimate $f(E)$ and $k_0(E)$ in the distributed activation energy model from three sets of experimental data," *Energy & Fuels* 9, 302-307. DOI: 10.1021/ef00050a014

Miura, K., and Maki, T. (1998). "A simple method for estimating $f(E)$ and $k_0(E)$ in the distributed activation energy model," *Energy & Fuels* 12, 864-869. DOI: 10.1021/ef970212q

Lazdovica, K., Kampars, V., Liepina, L., and Vilka, M. (2017). "Comparative study on thermal pyrolysis of buckwheat and wheat straws by using TGA-FTIR and Py-GC/MS methods," *Journal of Analytical and Applied Pyrolysis* 124, 1-15. DOI: 10.1016/j.jaap.2017.03.010

Liang, J., Lin, Y., Wu, S., Liu, C., Lei, M., and Zeng, C. (2015). "Enhancing the quality of bio-oil and selectivity of phenols compounds from pyrolysis of anaerobic digested

rice straw," *Bioresource Technology* 181, 220-223. DOI: 10.1016/j.biortech.2015.01.056

Li, Y., Zhang, R., He, Y., Zhang, C., Liu, X., Chen, C., and Liu, G. (2014). "Anaerobic co-digestion of chicken manure and corn stover in batch and continuously stirred tank reactor (CSTR)," *Bioresource Technology* 156, 342-347. DOI: 10.1016/j.biortech.2014.01.054

Li, X., Mei, Q., Dai, X., and Ding, G. (2017). "Effect of anaerobic digestion on sequential pyrolysis kinetics of organic solid wastes using thermogravimetric analysis and distributed activation energy model," *Bioresource Technology* 227, 297-307. DOI: 10.1016/j.biortech.2016.12.057

Ma, F., Zeng, Y., Wang, J., Yang, Y., Yang, X., and Zhang, X. (2013). "Thermogravimetric study and kinetic analysis of fungal pretreated corn stover using the distributed activation energy model," *Bioresource Technology* 128, 417-422. DOI: 10.1016/j.biortech.2012.10.144C

Manya, J., Velo, E., and Puigjaner, L. (2003). "Kinetics of biomass pyrolysis: A reformulated three parallel reactions model," *Industrial and Engineering Chemistry Research* 42(3), 434-441.DOI: 10.1021/ie020218p

Monlau, F., Sambusiti, C., Ficara, E., Aboulkas, A., Barakat, A., and Carrere, H. (2015a). "New opportunities for agricultural digestate valorization: Current situation and perspectives," *Energy & Environmental Science* 8(9), 2600-2621. DOI: 10.1039/c5ee01633ac

Monlau, F., Sambusiti, C., Antoniou, N., Barakat, A., and Zabaniotou, A. (2015b). "A new concept for enhancing energy recovery from agricultural residues by coupling anaerobic digestion and pyrolysis process," *Applied Energy* 148, 32-38. DOI: 10.1016/j.apenergy.2015.03.024C

Nassar, M. M. (1999). "Thermal analysis kinetics of bagasse and rice straw," *Energy Sources* 20(9), 831-837. DOI: 10.1080/00908319808970101

Neumann, J., Meyer, J., Ouadi, M., Apfelbacher, A., Binder, S., and Hornung, A. (2016). "The conversion of anaerobic digestion waste into biofuels via a novel thermo-catalytic reforming process," *Waste Management* 47(Pt A), 141-148. DOI: 10.1016/j.wasman.2015.07.001

Quan, C., Gao, N., and Song, Q. (2016). "Pyrolysis of biomass components in a TGA and a fixed bed reactor: Thermochemical behaviors, kinetics, and product characterization," *Journal of Analytical and Applied Pyrolysis* 121, 84-92. DOI: 10.1016/j.jaap.2016.07.005

Skodras, G., Grammelis, P., Basinas, P., Kakaras, E., and Sakellaropoulos, G. (2006). "Pyrolysis and combustion characteristics of biomass and wastederived feedstock," *Industrial and Engineering Chemistry Research* 45(11), 3791-3799. DOI: 10.1021/ie060107g

Soria-Verdugo, A., Garcia-Gutierrez, L. M., Blanco-Cano, L., Garcia-Hernando, N., and Ruiz-Rivas, U. (2014). "Evaluating the accuracy of the distributed activation energy model for biomass devolatilization curves obtained at high heating rates," *Energy Conversion and Management* 86, 1045-1049. DOI: 10.1016/j.enconman.2014.06.074

Tian, L., Shen, B., Xu, H., Li, F., Wang, Y., and Singh, S. (2016). "Thermal behavior of waste tea pyrolysis by TG-FTIR analysis," *Energy* 103, 533-542. DOI: 10.1016/j.energy.2016.03.022

Tihay, V., and Gillard, P. (2010). "Pyrolysis gases released during the thermal decomposition of three Mediterranean species," *Journal of Analytical and Applied*

Pyrolysis 88(2), 168-174. DOI: 10.1016/j.jaap.2010.04.002

Van Soest, P.J., Robertson, J.B., Lewis, B.A. (1991). "Methods for dietary fiber, neutral detergent fiber, and nonstarch polysaccharides in relation to animal nutrition," *Journal of Dairy Science* 74(10), 3583-3597. DOI: 10.3168/jds.S0022-0302(91)78551-2.

Wang, T., Ye, X., Yin, J., Jin, Z., Lu, Q., Zheng, Z., and Dong, C. (2014). "Fast pyrolysis product distribution of biopretreated corn stalk by methanogen," *Bioresource Technology* 169, 812-815. DOI: 10.1016/j.biortech.2014.07.074

Wang, S., Lin, H., Ru, B., Sun, W., Wang, Y., and Luo, Z. (2014). "Comparison of the pyrolysis behavior of pyrolytic lignin and milled wood lignin by using TG–FTIR analysis," *Journal of Analytical and Applied Pyrolysis* 108, 78-85. DOI: 10.1016/j.jaap.2014.05.014

Wang, S., Wang, K., Liu, Q., Gu, Y., Luo, Z., Cen, K., and Fransson, T. (2009). "Comparison of the pyrolysis behavior of lignins from different tree species," *Biotechnology Advances* 27(5), 562-567. DOI: 10.1016/j.biotechadv.2009.04.010

Yang, H., Yan, R., Chen, H., Dong, H. L., and Zheng, C. (2007). "Characteristics of hemicellulose, cellulose, and lignin pyrolysis," *Fuel* 86(12-13), 1781-1788. DOI: 10.1016/j.fuel.2006.12.013

Yao, Y., Gao, B., Inyang, M., Zimmerman, A. R., Cao, X., Pullammanappallil, P., and Yang, L. (2011). "Biochar derived from anaerobically digested sugar beet tailings: Characterization and phosphate removal potential," *Bioresource Technology* 102(10), 6273-6278. DOI: 10.1016/j.biortech.2011.03.006

Yuan, T., Tahmasebi, A., and Yu, J. (2015). "Comparative study on pyrolysis of lignocellulosic and algal biomass using a thermogravimetric and a fixed-bed reactor," *Bioresource Technology* 175, 333-341. DOI: 10.1016/j.biortech.2014.10.108